We thank the reviewer's further comments and suggestions, which will assist us in providing a more accurate description of our work. Our answers are listed in the following in red, after the referee's comments, which are in black. The modifications in the text are marked in yellow.

Editor:

The authors have addressed my initial major concern. I recommend this manuscript to be published after the authors revise a minor point.

It remains unconvinced why the transmittivity of HONO in the reference chamber is lower than that of O_3 even if I read your response.

According to JPL Publication 19-5, absorption cross section of ozone and quantum yield to form O(1D) at wavelengths of 390-410 is about 1 x 10^{-23} cm^2 and 0.08, respectively. On the other hand, Absorption cross section of HONO and photolysis quantum yield at wavelengths of 390-395 is the order of 10^{-21} cm^2 (two or three order of magnitude higher than that of ozone) and unity (about ten times higher than that of ozone), respectively.

The authors state "the spectral atlas of HONO was under wavelengths of 190-395 nm at 298 K, while that of O_3 was under wavelengths of 410-750 nm at 298 K". But the quantum yield to form O(1D) is 0 at wavelengths longer than 411 nm. The threshold wavelength of the photodissociation to form O(1D) is 411 nm in terms of binding energy of ozone.

In summary, I cannot believe the transmittivity of HONO in the reference chamber is lower than that of O_3.

Questions/Suggestions for improvement:

The authors should re-calculate *J* values and/or re-evaluate measurement errors.

The issue mentioned by reviewer is critical, sorry for the unclear description. The reviewer is correct that according to JPL Publication 19-5, absorption cross section of HONO at wavelengths of 390-395 ranged from ~ 4.0-17.1$\times10^{-21}$ cm^2, which is about two or three orders of magnitude higher than that of ozone (ranged from ~ 0.8-2.6 x 10^{-23} cm^2 at wavelengths of 390-410 nm), and the photolysis quantum yield of HONO at wavelengths of 390-395 is unity, which is about ten times higher than that of ozone (~ 0.08). This will surely make the *J* values of HONO inside the reference chamber (which only has sunlight with wavelengths > 390 nm) higher than that of ozone, according to the following equation:

$$J_{value\ TUV} = \int_a^b \delta_i \times \phi_i \times F_i \, \Delta\lambda_i$$

where *a* and *b* represent the range of the set wavelength, δ_i, ϕ_i, and F_i stand for the absorption cross section, quantum yield, and spectral actinic flux of the species *i*, respectively.

We also find that the transmittivity of HONO and O_3 in the reference chamber,

obtained from the TUV simulation as described in Sect. 3.2, were 0.01 and 0, respectively, which are shown in Table S13. Therefore, we believe the non-zero measurement results of the transmittivity of O_3 shown in Table 1 and Table S7 are mostly probably due to the instrument measurement error, this error is relatively large due to a limited number of measurement points (3 points for each species).

According to the working theory of the actinic flux spectrometer, the measurement error may rise from the angular response deviation of the quartz receiver head. According to Bohn et al. (2017), the measurement error of the actinic flux spectrometer can reach ±5 %. According to this, we re-evaluated the transmittivity error listed in Table 1 and Table S7 as follows: ① calculate the absolute measurement error of all measured *J* values inside and outside the reaction and reference chambers based on the ±5 % instrument measurement error; ② calculate the average values of all the measured *J* values (including ($J(NO_2)$, J(O1D), J(HONO), $J(H_2O_2)$, $J(NO_3\_M)$, $J(NO_3\_R)$, J(HCHO_M), and J(HCHO_R)) inside and outside the chambers; ③calculate the propagated error of transmittivity, using the following error propagation equation:

$$\sigma_{\text{Transmittivity}} = \sqrt{\left(\frac{\sigma_{J\ \text{value}\ \text{in}}}{A_{J\ \text{value}\ \text{in}}}\right)^2 + \left(\frac{\sigma_{J\ \text{value}\ \text{out}}}{A_{J\ \text{value}\ \text{out}}}\right)^2}$$

where $\sigma_{\text{Transmittivity}}$ represents the transmittivity error; $\sigma_{J\ \text{value}\ \text{in}}$ and $\sigma_{J\ \text{value}\ \text{out}}$ represent the measurement error of *J* value inside and outside the chambers, respectively; $A_{J\ \text{value}\ \text{in}}$ and $A_{J\ \text{value}\ \text{out}}$ represent the average *J* values measured inside and outside the chambers, respectively.

We find that the calculated transmittivity errors are 0.07 for all *J* values. Within this error range, the J(O1D), J(HONO), $J(H_2O_2)$, J(HCHO_M), and J(HCHO_R) can be considered statistically indistinguishable from 0 in the reference chamber, however, $J(NO_2)$, $J(NO_3\_M)$, and $J(NO_3\_R)$ still exhibit positive values.

To evaluate $P(O_3)_{net}$ error caused by the measurement error of *J* values, we introduced a ±5 % error to the measured *J* values during the 3rd stage of the 4-min simulation in method I, the modeled $P(O_3)_{net}$ results are added in Fig. S24 in the modified supplementary. We found that the inclusion of a -5 % *J* values measurement error can lead to a decrease in $P(O_3)_{net}$ by 7.27 %, while adding a +5 % *J* values measurement error can cause an increase in $P(O_3)_{net}$ by 3.08 %. This implies that the maximum bias of $P(O_3)_{net}$ caused by the measurement error of *J* values falls within the error range of the currently assessed $P(O_3)_{net}$ error, which was 13.9 % for method I. Therefore, we conclude that the transmittivity of HONO in the reference chamber is not statistically different from that of O_3 within the measurement error of *J* values, and this type of error will not influence our final modeling results and conclusions.

We have included the aforementioned analyses and revised the previous

inaccurate descriptions in the revised manuscript on page 11, lines 246-270:

"The photolysis frequencies of all species inside the reaction chamber were in agreement with those measured outside the reaction chamber within 4 %. Table S7 shows that the transmittivities of $J(H_2O_2)$, $J(NO_3\_M)$, $J(NO_3\_R)$, J(HCHO_M), and J(HCHO_R) in the reaction chamber were more than 90 %. However, we have observed that the transmittivities of $J(O^1D)$ were even higher than those of J(HONO) (as shown in Table 1) in the reference chamber (which blocks sunlight at wavelengths < 390 nm), theoretically, this is not possible according to JPL Publication 19-5 (Burkholder et al., 2020), where the absorption cross section of HONO at wavelengths of 390-395 ranged from approximately $4.0\text{-}17.1\times10^{-21}$ cm^2, which is about two or three orders of magnitude higher than that of ozone (which ranged from approximately $0.8\text{-}2.6\times10^{-23}$ cm^2 at wavelengths of 390-410 nm), and the photolysis quantum yield of HONO at wavelengths of 390-395 is unity, which is about ten times higher than that of ozone (~ 0.08). This will surely make the J values of HONO inside the reference chamber (which only has sunlight with wavelengths > 390 nm) higher than that of ozone, according to the Eq. (S9). We also found that the transmittivity of HONO and O_3 in the reference chamber obtained from the TUV simulation (as described in Sect. 3.2) were 0.01 and 0, respectively, as shown in Table S13. Therefore, we believe the non-zero measurement results of the transmittivity of O_3 shown in Table 1 and Table S7 are mostly probably due to the instrument measurement error, this error is relatively large due to a limit number of measurement points (3 points for each species). We further evaluated the measurement error of J values based on the instrument measurement error of the actinic flux spectrometer, which can reach ±5 % according to Bohn et al. (2017), and re-evaluated the transmittivity error listed in Table 1 and Table S7 following the procedures described in supplementary materials (Sect. 1.5). The calculation result from Eq. (S5) show that the transmittivities errors are 0.07 for all species, within this error range, J(O1D), J(HONO), $J(H_2O_2)$, J(HCHO_M), and J(HCHO_R) can be considered statistically indistinguishable from 0 in reference chamber. However, $J(NO_2)$, $J(NO_3\_M)$, and $J(NO_3\_R)$ still distinctly positive values. Specifically, the transmittivities of $J(NO_3\_M)$ and $J(NO_3\_R)$ of the reference chamber were more than 90 % (Table S7). The influence of the measurement error of J values of all species on $P(O_3)_{net}$ will be discussed in Sect. 3. "

And added the additional explanation in the modified supplementary on pages 12, lines 151-163:

"According to the working theory of the actinic flux spectrometer, the measurement error may rise from the angular response deviation of the quartz receiver head. According to Bohn et al. (2017), the measurement error of the actinic flux spectrometer can reach±5 %. According to this, we re-evaluated the transmittivity error listed in Table 1 and Table S7 as follows:①calculate the absolute measurement error of all measured *J* values inside and outside the reaction and reference chambers based on the ±5 % instrument measurement error; ②calculate the average values of all the measured *J* values (including ($J(NO_2)$, J(O1D), J(HONO), $J(H_2O_2)$, $J(NO_3\_M)$, $J(NO_3\_R)$, J(HCHO_M), and J(HCHO_R)) inside and outside the chambers; ③calculate the propagated error of transmittivity, using the following error propagation equation:

$$\sigma_{\text{Transmittivity}} = \sqrt{\left(\frac{\sigma_{J\ \text{value in}}}{A_{J\ \text{value in}}}\right)^2 + \left(\frac{\sigma_{J\ \text{value out}}}{A_{J\ \text{value out}}}\right)^2} \quad \text{(S5)}$$

where $\sigma_{\text{Transmittivity}}$ represents the transmittivity error; $\sigma_{J\ \text{value in}}$ and $\sigma_{J\ \text{value out}}$ represent the measurement error of *J* value inside and outside the chambers, respectively; $A_{J\ \text{value in}}$ and $A_{J\ \text{value out}}$ represent the average *J* values measured inside and outside the chambers, respectively."

And modified the caption of Table1 in the modified manuscript accordingly on page 12, lines 278-285:

"**Table 1. Transmittivities of photolysis frequency *J* (s^{-1}) values of different species in the reaction and reference chambers. The shaded and clear regions correspond to the transmittivities of *J* values in the reference (Ultem coated) and reaction (clear) chambers, respectively. The "transmittivities" column shows the transmittivities of the tested species from the measurements conducted with the set photolysis frequencies using SERIC XG-500B sunlight (this study) and ambient (literature). It should be noted that the errors listed here are relatively large and may not reliable due to a limit number of measurement points (3 points for each species). The calculated transmittivity errors are 0.07 for all species based on the ±5 % measurement error of the instrument.**"

As well as the caption of Table S7 in the modified supplementary materials on page 13, lines 165-172:

"**Table S7. Photolysis frequency *J* (s^{-1}) of different species and the transmittivities of *J* values in the reaction and reference chambers. The shaded and clear regions correspond to the photolysis frequencies and the transmittivities of *J* values in the reference (Ultem coated) and reaction (clear) chambers, respectively. The "transmittivities" column shows the transmittivities of the tested species from the measurements conducted with the set photolysis frequencies using SERIC XG-500B sunlight (this study) and ambient (literature). It should be noted that the errors listed here are relatively large and may not reliable due to a limit number of measurement points (3 points for each species). The calculated transmittivity errors are 0.07 for all species**

based on the ±5 % measurement error of the instrument."

Furthermore, $P(O_3)$net error caused by the ±5 % measurement error of *J* values during the 3rd stage of the 4-min simulation in method I are discussed in Sect. 3. in the modified manuscript on page 30, lines 682-689:

"To evaluate $P(O_3)_{net}$ error caused by the measurement error of *J* values, we introduced a ±5 % error to the measured *J* values during the 3rd stage of the 4-min simulation in method I. The modeled $P(O_3)_{net}$ results are presented in Fig. S24 in the supplementary materials. We observed that the inclusion of a -5 % measurement error in *J* values led to a decrease in $P(O_3)_{net}$ by 7.27 %, while adding a +5 % measurement error in *J* values caused an increase in $P(O_3)_{net}$ by 3.08 %. This implies that the maximum bias of $P(O_3)_{net}$ caused by the measurement error of *J* values falls within the error range of the currently assessed $P(O_3)_{net}$ error, which was 13.9 % for method I. Therefore, we conclude that this type of error will not influence our final modeling results and conclusions."

And the modeled $P(O_3)_{net}$ results are added in Fig. S24 in the modified supplementary materials on page 31, lines 395-399:

"

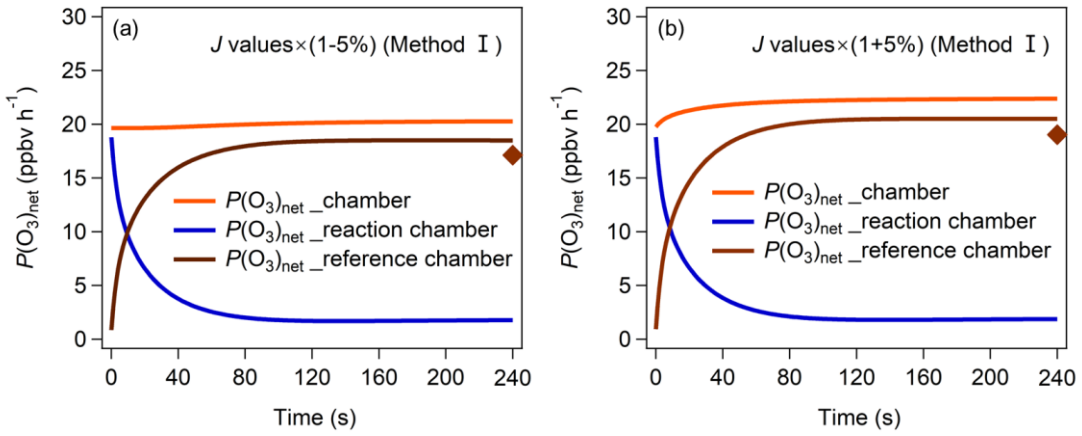

Figure S24: $P(O_3)_{net}$ changing in the reaction and reference chambers in method I with ± 5 % of measured *J* values."

Appendix:

We detected an error in the Supplementary Materials Table S12. The equation of measured *J* values used in the model simulation for Method II was incorrectly written, which we have now corrected. It is important to note that this didn't

influence any of our analyses results as we used the correct equation throughout all our analyses.

"**Table S12. *J* values used in the model simulation in reaction and reference chambers.**

	J values used in the model simulation	
	Measured *J* values: $J(NO_2)$, $J(O^1D)$, $J(HONO)$, $J(H_2O_2)$, $J(NO_3\_M)$, $J(NO_3\_R)$, $J(HCHO\_M)$, $J(HCHO\_R)$	Unmeasured *J* values: $J(HNO_3)$, $J(CH_3CHO)$, $J(MACR)$, $J(MEK)$, $J(HOCH_2CHO)$, $J(C_2H_5CHO)$, $J(C_3H_7CHO)$, $J(C_4H_9CHO)$, etc.
Method I	$J_{\text{trans measured}} \times J_{\text{value measured}}$	$J_{\text{trans TUV}} \times J_{\text{NO2 measured}} / J_{\text{NO2TUV}} \times J_{\text{valueTUV}}$
Method II	$J_{\text{trans TUV}} \times J_{\text{value measured}}$	$J_{\text{trans TUV}} \times J_{\text{NO2 measured}} / J_{\text{NO2TUV}} \times J_{\text{valueTUV}}$

"

References

Bohn B, Lohse I. Calibration and evaluation of CCD spectroradiometers for ground-based and airborne measurements of spectral actinic flux densities. Atmos. Meas. Tech., 10, 3151–3174, https://doi.org/10.5194/amt-10-3151-2017, 2017.

Burkholder, J., Sander, S., Abbatt, J., Barker, J., Cappa, C., Crounse, J., Dibble, T., Huie, R., Kolb, C., and Kurylo, M.: Chemical kinetics and photochemical data for use in atmospheric studies, evaluation number 19, Pasadena, CA: Jet Propulsion Laboratory, National Aeronautics and Space Administration, 2020, http://jpldataeval.jpl.nasa.gov. 2020.